Impedance and Magnetohydrodynamic Measurements for Label Free Detection and Differentiation of *E. Coli* and *S. Aureus* Using Magnetic Nanoparticles

Zeeshan, K. S. Daya, Prem Saran Tirumalai, and Evangelyn Alocilja, *Member, IEEE*

Abstract—In this paper, we used the distinguishable surface charge and mass of different bacterial strains for label free detection and differentiation of pathogen through impedance and magnetohydrodynamic (MHD) analysis. For the isolation of *Escherichia coli* and *Staphylococcus aureus*, functionalized magnetic nanoparticles (MNPs) were used. The proposed method is aimed at minimizing extensive chemical preparation and labor intensive conventional microbiological processing thereby reducing the detection time. Pathogens isolated from broth cultures using the MNPs were subjected to impedance rate measurement through an arduino-based automated impedance sensor along with differentiation on the basis of Larmor's motion through the MHD approach. The proposed method evidently reports that the two bacterial species bind differently to the MNPs giving appreciable variation in the impedance rate increment for a dc electric field of 250V/m. In addition to this, cross-field drift through 171.4 V/m electric field and a normal magnetic field of 500 Gauss led to lump formation in *S. aureus* but had no such effect on *E. coli*. The mobility analysis of the two species of bacteria was also carried out by observing the gyration of bacteria through naked eyes. The mobility of lumped bodies of *S. aureus* was of the order 10^{-10} m^2/V · sec; whereas for dispersed *E. coli*, it was 10^{-08} m^2/V · sec.

Index Terms—Index Terms- Label free, magnetic nanoparticles (MNPs), magnetohydrodynamics (MHD).

I. INTRODUCTION

DESPITE new developments in diagnostics, long turnaround time continues to be the major challenge in deciding the course of treatment for infectious diseases, claiming

7 million lives every year [1]. Unavailability of rapid detection methods has been a major cause for increased usage of broad-spectrum antibiotics forming superbugs [2]–[4]. Symbiosis of nanotechnology and life sciences has given way to new horizon of interdisciplinary rapid detection methods for cells and microorganisms [5], [6]. For characterizing different bacteria, researchers are trying to find a viable solution through optics [7], [8], by manipulating microfluidic channels [9], [10], through DNA antimicrobial peptide binding [11], by applying electrophoretic mobility and zeta potential analysis, etc. [12]–[14]. Although reliable, sample preparation and amplification [15]–[19] limit the efficacy of these techniques. Electronic nose for detection of bacteria in wound infections, basically a gas sensor especially designed to detect volatile organic compounds released by bacteria in a sample with recognition rate up to 96% does not involve amplification and rigorous sample preparation and its specificity to certain microorganisms serves as added attribute [20], but not being able to differentiate different pathogens limits its usage as replacement for conventional techniques. ZnO based nano-biosensors take advantage of small sized nanorods for determining the concentration of extracellular biomolecules. Nanorod based sensors successfully detected *S. pneumonia* and *E. coli* in drinking water [21], [22]. Rapid dielectric characterization of cells that included RBCs and micro beads of polystyrene has been reported in [10] where different cells were characterized for their electrical properties through micro fabricated flow cytometer. Impedance spectroscopy has recently emerged as the most reveled method of detection in which researchers are putting serious contributions [23]. One fundamental reason being that Impedance spectroscopy does not depend on extensive treatment of sample before subjecting to analysis [24]. Other sensors that deserve mentioning for their unique features are those based on SERS (Surface Enhanced Raman Scattering) and LAPS (Light-Addressable Potentiometric Sensor), SERS based sensors are equipped with excellent portability and detection limit up to 100 CFU ml^{-1} [6] but detection time of 4 hours keeps the issue of rapid detection far from settled. LAPS based sensors have a unique advantage of spatially exciting the surface of the sensor for detection of bioactivity, these sensors focus on the
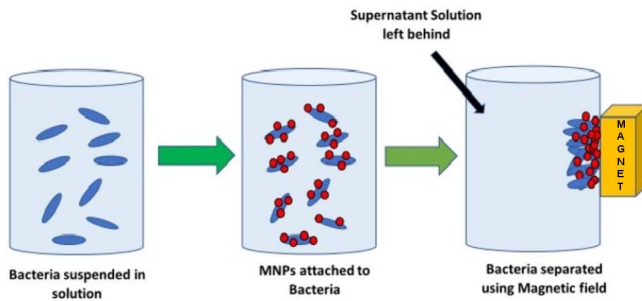
Fig. 1. Schematic of process followed for MNPs assisted bacterial separation.

molecular and chemical changes due to metabolic activities. LAPS based sensors show high sensitivity, but the purpose of differentiation has not been addressed yet [8].

In this paper, a technique for rapid detection and differentiation of *E. coli* and *S. aureus* is discussed based on the specific difference in the adherence properties of the bacteria to MNPs. A sensor is developed to track impedance rate-analysis. In addition to impedance measurement, another confirmatory and unique technique based on Magnetohydrodynamics (MHD) is also proposed which utilizes the surface charge negativity of the bacteria [25] in the presence of orthogonal electric and magnetic field. The unique surface charge and mass of the bacterial strain gives different gyration frequency and radius in the presence of electric and magnetic field. This unique approach can also find potential application in multiplexed sensor for detection and differentiation of multiple pathogens in food and clinical samples giving an alternative to conventional tedious microbiological methods without any prior sample treatment and processing.

II. DETAILS OF THE EXPERIMENT

A. Using MNPs in the Isolation of Pathogens

The technique of bacterial separation is the same as used by many researchers [26], [27] that includes adhering of MNPs to the surface of bacteria due to action of functional group and then extracting out the supernatant using magnetic field (Fig.1). These Glycan-coated magnetic nanoparticles were provided by the Alocilja Research Group from Michigan State University (East Lansing, USA).

These MNPs consist of magnetite (Fe_3O_4) in the core with a glycan (chitosan) shell. The superparamagnetic iron oxide nanoparticles have an average size of 99±58 nm with zero average magnetization in the absence of magnetic field, but an external field is able to magnetize them. Fig.1 shows the schematic of the experimental setup for isolation of pathogens and Fig.2 shows a transmission electron microscope (TEM) image of *E. coli* with MNP capture. The clumps of *S. aureus* were observed through optical microscope at 100X zoom as shown in Fig.3. A good confirmation for the binding action of the MNPs utilised in the present work can be reviewed from Lim *et. al* [28]. All experiments were performed with the bacterial cultures that were inoculated in Tryptone Soy Broth (TSB) and incubated for 24 hours.The bacterial strains
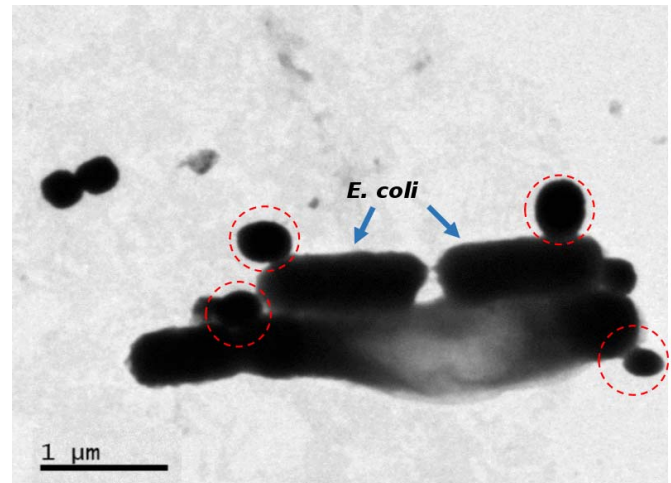

Fig. 2. Transmission Electron Microscope (TEM) image of *E. coli* (pointed with blue arrow) captured with MNPs (highlighted in dotted circle) taken by Alocilja Research Group, Michigan State University.
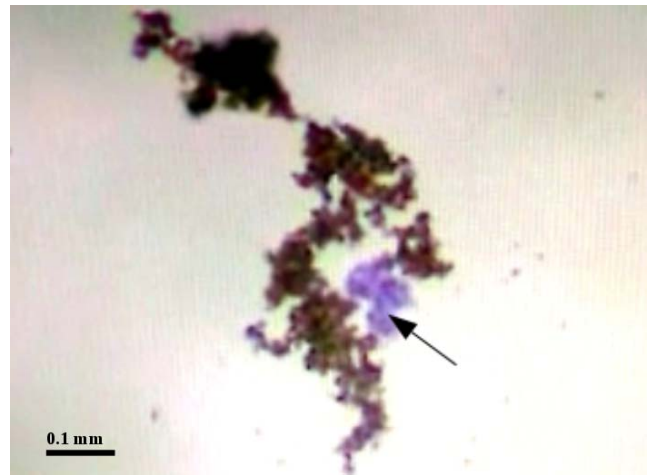

Fig. 3. Clumps of *S. aureus* stained with crystal violet (pointed by an arrow) surrounded by MNPs seen through optical microscope under 100X zoom.

were obtained from the National Collection of Industrial Microbes (NCIM) Resource Centre, Pune, India.

B. Impedance Rate-Analyser

The design specifications of the impedance rate analyser are shown in Fig.4, comprising of a glass tube with graphite electrodes in which the sample was filled. The spacing between the electrodes was 2 cm for the potential difference of 5 V giving a d.c. electric field of 250 V/m. A bar magnet with flux density between 10 and 20 Gauss was placed vertically across the centre of the tube with spacing of 1.5 cm. Utilizing the fact that both *E. coli* and *S. aureus* have negative charge accumulated on its surface [25] when a d.c. electric field is applied, the bacteria move towards the positive electrode. If these bacteria are made to adhere to MNPs, then subjecting a magnetic field reduces the speed of bacteria towards the positive electrode because the MNPs are influenced by the magnetic field [27] and hence increases the impedance of
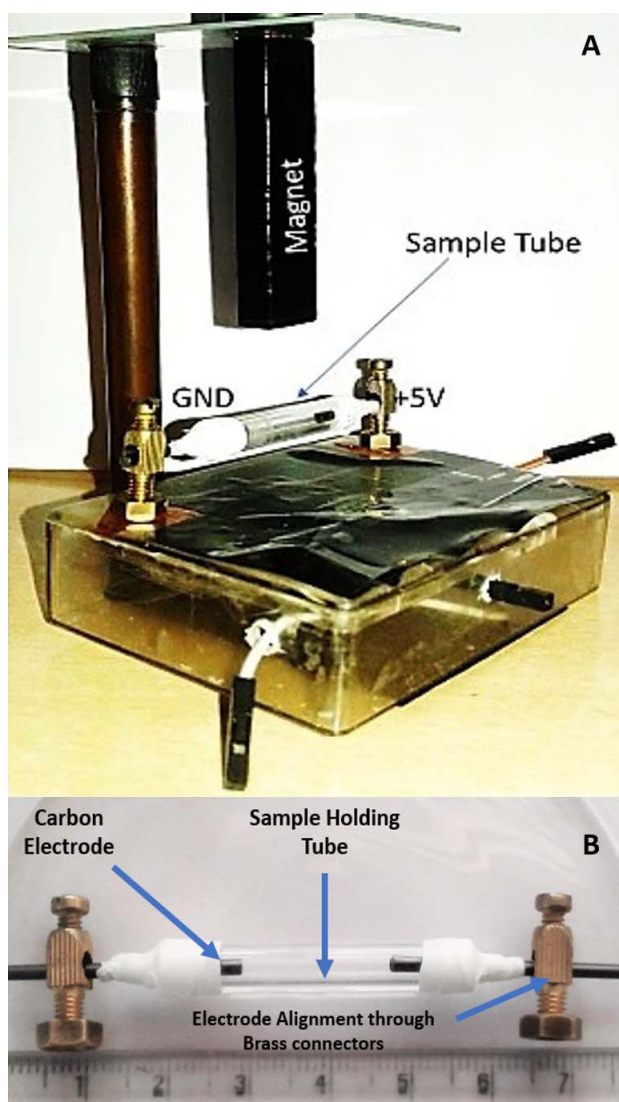
Fig. 4. A) Specification of sensor design showing the teflon-taped end of the sample tube with graphite electrodes and simultaneous action of electric and magnetic field. B) Detailed view of sample holding tube.
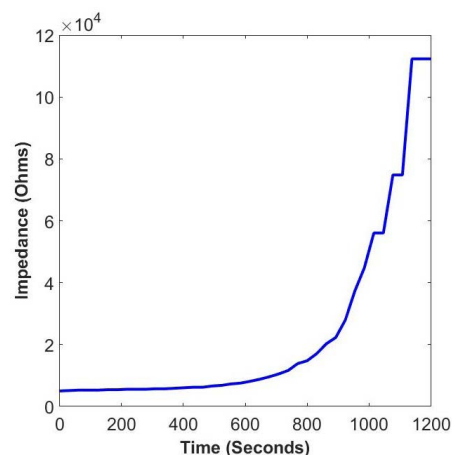

Fig. 5. Day:1 Variation of impedance of 0.85% by weight solution of NaCl (Time on x-axis sampled every 30 seconds to give 40 readings over 20 minutes).
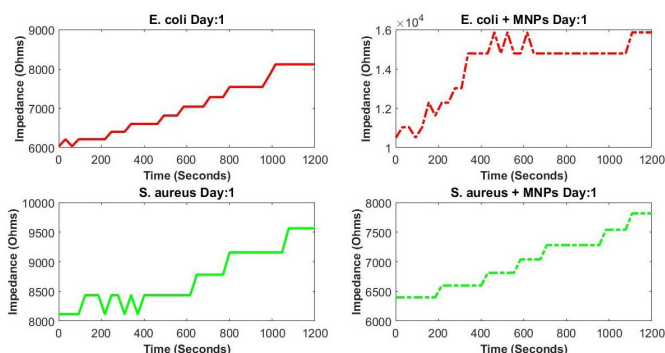

Fig. 6. Variation of Impedance with respect to time sampled every 30 seconds to give 40 readings over 20 minutes for Day 1- Top Left (2ml suspension of *E. coli*), Top Right (*E. coli* added with 20μl of MNPs), Bottom Left (2ml suspension of *S. aureus*), Bottom Right (*S. aureus* added with 20μl of MNPs).

Fig. 7. Variation of Impedance with respect to time sampled every 30 seconds to give 40 readings over 20 minutes for Day 2- Top Left (2ml suspension of *E. coli*), Top Right (*E. coli* added with 20μl of MNPs), Bottom Left (2ml suspension of *S. aureus*), Bottom Right (*S. aureus* added with 20μl of MNPs).

the sample tube. The impedance was monitored through an arduino interface across a potential divider circuit obtained by connecting a known resistance of 10 kΩ in series with the sample tube and the readings were noted every second for twenty minutes. The graphs depicted in Fig.6 and Fig.7 were plotted for analysis of impedance over the period of 20 minutes i.e. 1200 seconds, sampled at every 30 seconds to give 40 readings. The average rate of change of impedance for both cultures, with and without MNP capture, was calculated by averaging those 40 readings. Fig.5 shows the time versus impedance graph of saline. Due to large number of ions present in 0.85 % by weight solution of NaCl, the impedance increases from few ohms to hundred kilo-ohms, the variation of impedance of saline was measured for Day 1 only to check the sampling frequency of the designed sensor and to check for outliers in data. Fig.6 and Fig.7 show the variation of impedance with time for both cultures measured on two different days. Since the binding of the two bacteria to MNPs

was different, the change in impedance rate was due to the effect of adding MNPs to their cultures resulting in a uniquely different pattern for the two species as summarized in Table I and in Table II on the basis of data obtained for Day 1 and Day 2 from independently cultured samples. In the presence

TABLE I
COMPARISON OF VARIATION IN IMPEDANCE ON ADDING MNPS
TO THE BACTERIAL CULTURES FOR DAY 1

Sample Name	Resistance Slope (Ω / second)
Saline	$3.5 *10^3$
E. coli	69
E. coli + MNPs	178.61
S. aureus	48.32
S. aureus +MNPs	47.28

TABLE II
COMPARISON OF VARIATION IN IMPEDANCE ON ADDING MNPS
TO THE BACTERIAL CULTURES FOR DAY 2

Sample Name	Resistance Slope (Ω / second)
Saline	—-
E. coli	104.84
E. coli + MNPs	169.68
S. aureus	76.107
S. aureus+MNPs	75.777

of a magnetic field, the resistance for *E. coli* increased in an appreciable amount contrary to the case of *S. aureus* where negligible changes were observed. This phenomenon could be attributed to their variation in size. *E. coli* is a Gram-negative rod-shaped bacterium estimated to be 3μm in length and 1μm in diameter [29]. Furthermore, *E. coli* have flagellar filaments that are several μm long and 20 nm in diameter [30]. On the other hand, *S. aureus* is a Gram-positive non-flagellated bacterium that is spherical in shape with an estimated diameter of less than 1μm [31], [32]. Hence, *E. coli* is much larger than *S. aureus* that could have added to the drag on *E. coli* against the magnetohydrodynamic force (see Fig.8). Additionally, *E. coli* has more negative surface charge and less soft surface than *S. aureus* [32], [33]. Step-increment with oscillations in the impedance is due to the effect of magnetic field on the charged bacterial surface and size. Sudden increment followed by fall in the value of impedance incurs the hall-type effect of magnetic field on motion of bacteria under electric drift due to the negative surface charge. To further understand the effect of magnetic action as a confirmatory differentiation process, detailed analysis is done based on magnetohydrodynamic approach as described in the next section.

C. Magnetohydrodynamic Approach for Detection

In this section of the experiment, we applied the Lorentz force based hydrodynamics [9] to the concerned bacterial species. In the magnetohydrodynamics approach, the bacteria are brought to the action of simultaneous drift (E x B) due to the action of Lorentz force on the circular motion of the charged bodies [34]. The Larmor's radius and the cyclotron frequency of the circular motion of the gyrating bodies depend on the mass and the charge of these species. Different bacterial species can be differentiated by determining the charge-to-mass ratio. Mobility of cells in the presence of the (E x B) drift contains both the information about charge and about mass as well. Instead of applying the Doppler's velocimetry approach to find out the mobility [13], we have used the action of MHD forces on the bacteria, which relates cyclotron frequency to
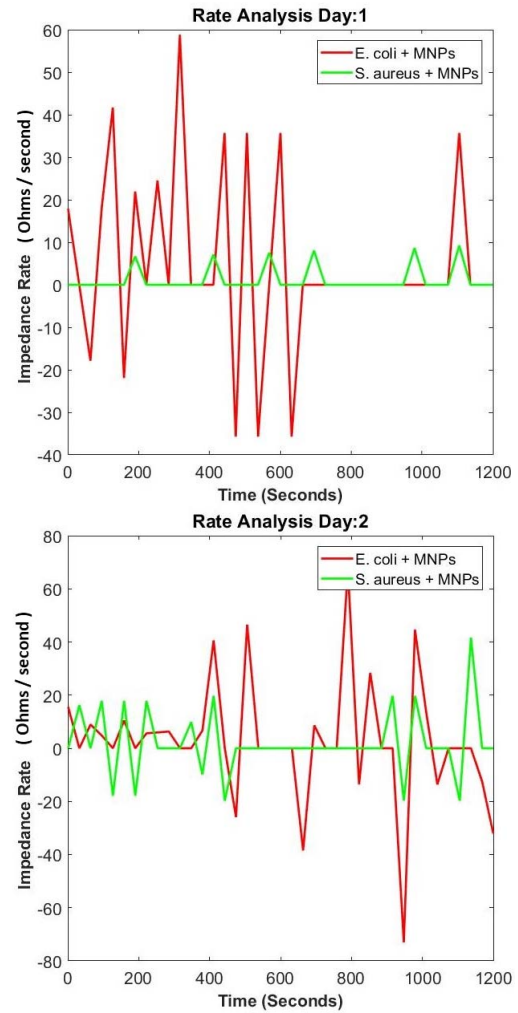

Fig. 8. Comparison of rate of Impedance change for *E. coli* & *S. aureus*.

Lorentz force.

$$qvB = mv^2/r \tag{1}$$
$$v = \mu E \tag{2}$$

From equations (1) and (2) above, one can derive equation (3) utilising the fact that $v=r\omega$ for circular motion.

$$\mu = qBr/mE \tag{3}$$

The mobility analysis for *S. aureus* can be done without use of any magnifying aid or stereo zooming. This was possible due to the bunch forming tendency of *S. aureus* in the presence of E x B field. The cultures were stained using safranin dye and because of cell clumping, big colonies (so big to be able to be seen with naked eye) were formed and their gyrations were observed for radius and period of revolution. Assuming the size of a bacterium to be 1μm and mass to be 1 picogram [35], it can be asserted that a 1 mm lump comprises of 1,000 bacterial cells and its average mass being 1,000 picograms. The radius (r) and time-period (T) were observed for selected lumps performing gyration. The parameters selected were B = 500 Gauss i.e. 0.05 Tesla and a constant electric field was applied through a potential
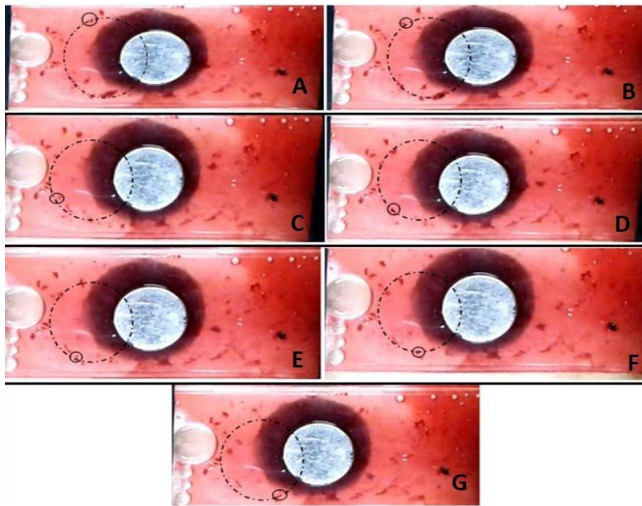
Fig. 9. Observation of the moving lump in the presence of Lorentz force field (A-G). The dotted circle traces the path of the lumped cell formed by clumping of bacteria and the small circle on this dotted circle keeps the particle in sight.

TABLE III
OBSERVED LARMOUR RADIUS AND FREQUENCY

Size of Lump/ No. of Bacterial Cells	Larmour Radius (r) in cm	Frequency (ω) rad.sec^{-1}
2 mm/2000 cells	1.5	0.3925
3 mm/3000 cells	1.0	0.3140
5 mm/5000 cells	2.0	0.0785

TABLE IV
CALCULATED CHARGE AND MOBILITY

No. of Bacterial Cells	Charge (q)	Mobility (μ) m^2/V.sec
2000 cells	$9.8*10^6$e	$34.3*10^{-10}$
3000 cells	$11.78*10^6$e	$18.33*10^{-10}$
5000 cells	$4.9*10^6$e	$9.148*10^{-10}$

difference of 12 V over a distance of 7 cm hence, giving E = 171.4V/m. Fig.9 shows the observation of the moving lump in the presence of Lorentz force field. The size of the particle was noted and its radius and period of revolution were observed. The dotted circle traces the path of the lumped cell and a small circle on this dotted circle keeps the particle in sight. The analysis is done for particle of three different sizes of lumped *S. aureus*: 2 mm, 3 mm and 5 mm. The observed radius and frequency of revolution depending on the periodic revolution of the mentioned particles are tabulted in Table III. The charge (q) and the mobility (μ) were calculated as shown in Table IV. Moreover, in comparison to the mobility as reported in [13] using zeta potential Doppler shift velocimetry for single entity of *S. aureus*, the mobility is of the order of 10^{-08} m^2/V.sec. It can be argued that the factor of 100 is due to the effect of lump formation of *S. aureus*. It is quiet difi'cult to say anything about the trend of the variation due to charge but a generic trend is observed in the mobility as depicted in Fig.10 showing inverse relation between mobility and size.

Since no lump formation is observed in the case of *E. coli*, an indirect approach was used, as shown in Table IV. For a single bacterium, the charge will be less by a factor of 1,000.
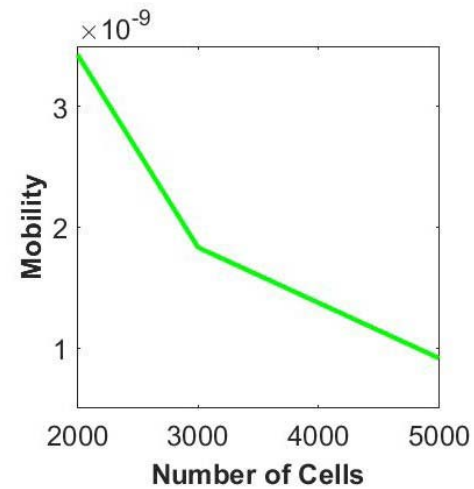

Fig. 10. Variation of mobility with respect to increase in number of cell clumping.

Fig. 11. *E. coli* gyrations subjected to ExB drift after staining with safranin. The arrow direction signifies the effect of north and south poles.

On average, a single bacterium of *E. coli* would have a surface charge of the order of 10^3e (nearly 10^{-15} Coulombs) where e is charge of one electron. Using equation (3), the average mobility of the single *E. coli* was calculated. For E = 171.4 V/s and B = 0.05 T. The mobility comes out to be in the range $29*10^{-08}$ to $58*10^{-08}$ m^2/V.sec for the observed radius between 1-2 cm as shown in Fig.11. The order of the mobility (10^{-08}) is comparable to the mobility of *E. coli* as reported in [13]. Hence this method of MHD based gyration seems to be helpful in characteristically differentiating bacteria without going through any bulk processing or intense chemical preparation or isolation from the suspected sample.

III. CONCLUSIONS

The proposed method for label-free detection and differentiation of bacteria is a promising solution to the problem of rapid detection and differentiation of bacteria. The described methods aim at cutting down the conventional micro-biological

approaches of bacterial detection involving grueling chemical assistance. Natural tendency of *S. aureus* to form lumps, served as an additional advantage of the proposed differentiation technique. The agreement of the mobility parameter to the previously reported value [13], [36], [37] accounts for the reliability of the results obtained by the proposed technique of detection. The best feature of the proposed technique is the turn around time: for resistance analysis, 20 minutes are required for data acquisition and in the case of MHD approach, instant results are obtained. This makes the presented technique fast, viable and reliable for fabricating a sensor that can be used as a table top detection system which would not require any expert assistance. In case of pathogenic infections, early treatment requires fast detection. Current methods take long time for diagnosis and prognosis, the work proposed here provides an option for rapid and specific diagnosis of bacterial pathogens.

REFERENCES

[1] (Jan. 2017). *World Health Statistics 2015. World Health Organisation—The Top 10 Causes of Death Fact Sheet*. [Online]. Available: http://www.who.int/mediacentre/factsheets/fs310/en/

[2] P. Nordmann, T. Naas, N. Fortineau, and L. Poirel, "Superbugs in the coming new decade; multidrug resistance and prospects for treatment of *Staphylococcus aureus, Enterococcus spp.* and *Pseudomonas aeruginosa* in 2010," *Current Opinion Microbiol.*, vol. 10, no. 5, pp. 436–440, 2007.

[3] B. M. Kuehn, "Antibiotic-resistant 'superbugs' may be transmitted from animals to humans," *JAMA*, vol. 298, no. 18, pp. 2125–2126, 2007.

[4] B. Spellberg *et al.*, "The epidemic of antibiotic-resistant infections: A call to action for the medical community from the infectious diseases society of America," *Clin. Infectious Diseases*, vol. 46, no. 2, pp. 155–164, 2008.

[5] R. Bashir, R. Gomez, H. Li, D. Akin, and A. Gupta, "Interfacing micro/nanotechnology with life-sciences for detection of cells and microorganisms," in *Proc. Bipolar/BiCMOS Circuits Technol. Meeting*, 2003, pp. 157–160.

[6] X. Wu, C. Xu, R. A. Tripp, Y.-W. Huang, and Y. Zhao, "Detection and differentiation of foodborne pathogenic bacteria in mung bean sprouts using field deployable label-free SERS devices," *Analyst*, vol. 138, no. 10, pp. 3005–3012, 2013.

[7] O. Efe and T. Yildirim, "Assessment of optical detection methods for compact biosensors," in *Proc. Med. Technol. Nat. Congr. (TIPTEKNO)*, Trabzon, Turkey, Oct. 2017, pp. 1–4.

[8] T. Wagner *et al.*, "Light-addressable potentiometric sensor (LAPS) combined with magnetic beads for pharmaceutical screening," *Phys. Med.*, vol. 1, pp. 2–7, Jun. 2016.

[9] O.-T. Son, J.-H. Park, C.-G. Lee, C. Lee, and H.-I. Jung, "Manipulation of phospholiposome in microfluidic channel using lorentz force," in *Proc. 2nd IEEE Int. Conf. Nano/Micro Eng. Mol. Syst.*, Bangkok, Thailand, Jan. 2007, pp. 552–555.

[10] K. Cheung, S. Gawad, and P. Renaud, "Impedance spectroscopy flow cytometry: On-chip label-free cell differentiation," *Cytometry A*, vol. 65, no. 2, pp. 124–132, 2005.

[11] P. Fojan, K. R. Jensen, and L. Gurevich, "Label-free detection of biomolecular interaction—DNA—Antimicrobial peptide binding," in *Proc. 2nd Int. Conf. Wireless Commun., Veh. Technol., Inf. Theory Aerosp. Electron. Syst. Technol. (Wireless VITAE)*, Chennai, India, Feb./Mar. 2011, pp. 1–5.

[12] N. Takahashi, A. Aki, T. Ukai, Y. Nakajima, T. Maekawa, and T. Hanajiri, "Electrophoretic mobility and resultant zeta potential of an individual cell analyzed by electrophoretic coulter method," in *Proc. Int. Semiconductor Device Res. Symp.*, College Park, MD, USA, Dec. 2009, pp. 1–2.

[13] L. P. Foong, "Electrophoretic studies of surface charge on unicellular bacteria," Ph.D. dissertation, Faculty of Sci., Univ. Malaya, Kuala Lumpur, Malaysia, 2009.

[14] S. Halder *et al.*, "Alteration of Zeta potential and membrane permeability in bacteria: A study with cationic agents," *SpringerPlus*, vol. 4, no. 1, 2015, Art. no. 672.

[15] S. Kim, G. Yu, T. Kim, K. Shin, and J. Yoon, "Rapid bacterial detection with an interdigitated array electrode by electrochemical impedance spectroscopy," *Electrochimica Acta*, vol. 82, pp. 126–131, Nov. 2012.

[16] M. Zourob, S. Elwary, and A. P. F. Turner, Eds., *Principles of Bacterial Detection: Biosensors, Recognition Receptors and Microsystems*. Berlin, Germany: Springer, 2008.

[17] V. Nandakumar, D. Bishop, E. Alonas, J. LaBelle, L. Joshi, and T. L. Alford, "A low-cost electrochemical biosensor for rapid bacterial detection," *IEEE Sensors J.*, vol. 11, no. 1, pp. 210–216, Jan. 2011.

[18] L. E. Lehmann *et al.*, "A multiplex real-time PCR assay for rapid detection and differentiation of 25 bacterial and fungal pathogens from whole blood samples," *Med. Microbiol. Immunol.*, vol. 197, no. 3, pp. 313–324, 2008.

[19] E. Meylan, J. Tschopp, and M. Karin, "Intracellular pattern recognition receptors in the host response," *Nature*, vol. 442, no. 7098, pp. 39–44, 2006.

[20] H. Sun *et al.*, "Sensor array optimization of electronic nose for detection of bacteria in wound infection," *IEEE Trans. Ind. Electron.*, vol. 64, no. 9, pp. 7350–7358, Sep. 2017.

[21] R. Borgohain and S. Baruah, "Development and testing of ZnO nanorods based biosensor on model gram-positive and Gram-negative bacteria," *IEEE Sensors J.*, vol. 17, no. 9, pp. 2649–2653, May 2017.

[22] H. A. Wahab, A. A. Salama, A. A. El Saied, M. Willander, O. Nur, and I. K. Battisha, "Zinc oxide nano-rods based glucose biosensor devices fabrication," *Results Phys.*, vol. 9, pp. 809–814, Jun. 2018.

[23] D. Ortiz-Aguayo and M. del Valle, "Label-free aptasensor for lysozyme detection using electrochemical impedance spectroscopy," *Sensors*, vol. 18, no. 2, p. 354, 2018.

[24] C. Küttel *et al.*, "Label-free detection of *Babesia bovis* infected red blood cells using impedance spectroscopy on a microfabricated flow cytometer," *Acta Tropica*, vol. 102, no. 1, pp. 63–68, 2007.

[25] J. S. Dickson and M. Koohmaraie, "Cell surface charge characteristics and their relationship to bacterial attachment to meat surfaces," *Appl. Environ. Microbiol.*, vol. 55, no. 4, pp. 832–836, 1989.

[26] H. Gu, K. Xu, C. Xu, and B. Xu, "Biofunctional magnetic nanoparticles for protein separation and pathogen detection," *Chem. Commun.*, vol. 9, no. 9, pp. 941–949, 2006.

[27] Q. A. Pankhurst, J. Connolly, S. K. Jones, and J. Dobson, "Applications of magnetic nanoparticles in biomedicine," *J. Phys. D, Appl. Phys.*, vol. 36, no. 13, p. R167, 2003.

[28] D. Lim *et al.*, "Alocilja magnetic nanoparticles capture *Escherichia coli* O157:H7 isolates," *Philippine J. Pathol. Open Access*, vol. 2, no. 2, pp. 47–49, 2017.

[29] G. Reshes, S. Vanounou, I. Fishov, and M. Feingold, "Cell shape dynamics in *Escherichia coli*," *Biophys. J.*, vol. 94, no. 1, pp. 251–264, 2008.

[30] S. Chattopadhyay, R. Moldovan, C. Yeung, and X. L. Wu, "Swimming efficiency of bacterium *Escherichiacoli*," *Proc. Nat. Acad. Sci. USA*, vol. 103, no. 37, pp. 13712–13717, 2006.

[31] J. M. Monteiro *et al.*, "Cell shape dynamics during the staphylococcal cell cycle," *Nature Commun.*, vol. 6, Aug. 2015, Art. no. 8055.

[32] C. Kaito and K. Sekimizu, "Colony spreading in *Staphylococcus aureus*," *J. Bacteriol.*, vol. 189, no. 6, pp. 2553–2557, 2007.

[33] R. Sonohara, N. Muramatsu, H. Ohshima, and T. Kondo, "Difference in surface properties between *Escherichia coli* and *Staphylococcus aureus* as revealed by electrophoretic mobility measurements," *Biophys. Chem.*, vol. 55, no. 3, pp. 273–277, 1995.

[34] K. V. Roberts and J. B. Taylor, "Magnetohydrodynamic equations for finite Larmor radius," *Phys. Rev. Lett.*, vol. 8, no. 5, p. 197, 1962.

[35] *Mass of Bacterium—Hypertextbook- the Physics Textbook*. [Online]. Available: https://hypertextbook.com/facts/2003/LouisSiu.shtml

[36] A. Pfetsch and T. Welsch, "Determination of the electrophoretic mobility of bacteria and their separation by capillary zone electrophoresis," *Fresenius' J. Anal. Chem.*, vol. 359, no. 2, pp. 198–201, 1997.

[37] M. E. Bayer and J. L. Sloyer, Jr., "The electrophoretic mobility of Gram-negative and gram-positive bacteria: An electrokinetic analysis," *Microbiology*, vol. 136, no. 5, pp. 867–874, 1990.